

## Photon-photon resonances in quantum electrodynamics

Jurij W. Darewych, Marko Horbatsch, and Roman Koniuk  
*Physics Department, York University, Toronto, Ontario, M3J 1P3 Canada*  
 (Received 11 March 1991)

A Hamiltonian variational method is used in quantum field theory to describe photon-photon scattering in quantum electrodynamics (QED) at energies where the cross section is dominated by the formation of positronium states of symmetry  $J^{PC}=0^{-+}$ . It is shown how the originally homogeneous eigenvalue equation for the positronium bound states is augmented by an inhomogeneity due to the coupling to the two-photon sector. Thus our calculation reproduces the well-known result that QED has a continuous spectrum at all energies and that the positronium bound states appear as resonances in the  $\gamma\text{-}\gamma$  scattering channel. Consequences for photon-photon scattering experiments are discussed briefly.

PACS number(s): 12.20.Ds, 11.10.St, 11.15.Tk

### I. INTRODUCTION

It has become a standard phrase to say that quantum electrodynamics (QED) is the most successful theory known, in that it is in spectacular agreement with experimental observation. (In the case of the electron's magnetic moment this agreement is better than ten decimal figures [1].) Yet one of the fundamental QED processes, that of photon-photon scattering, which, in lowest order, proceeds via virtual electron-positron pairs [2], has eluded direct experimental verification to date. The reasons for this are fairly obvious: the cross section for photon-photon scattering is, except at resonant energies, very small, and the difficulties of performing high-intensity colliding-beam experiments are considerable. With the recent development of laser technology, however, such experiments are now practical, and are being discussed in the literature [3].

The photon-photon scattering cross section, at lowest order in perturbation theory was calculated long ago [4,2], and yields the low-energy ( $\hbar\omega \ll mc^2$ ) result

$$\sigma_{\gamma\gamma \rightarrow \gamma\gamma} = \frac{973}{10125} \frac{\alpha^2}{\pi^2} r_0^2 \left[ \frac{\hbar\omega}{mc^2} \right]^6 \quad (1)$$

for the elastic cross section of unpolarized photons. Here,  $\alpha$  is the QED fine-structure constant,  $m$  is the electron mass,  $r_0 = e^2/mc^2$  the classical electron radius, and  $\omega$  the photon center-of-mass energy. The interest in this process is, however, not at low energies, but in the region  $\hbar\omega \simeq mc^2$ , where the cross section becomes quite substantial, reaching the  $\mu b$  regime [3]. Indeed, on resonance the cross section reaches the unitary limit, as has been pointed out by Guzenko and Fomin [5], and is given by (here and henceforth we set  $\hbar=c=1$ )

$$\sigma = 2\pi/m^2 \approx 10^{-20} \text{ cm}^2. \quad (2)$$

Recently [6], we have pointed out, using scalar QED as a pedagogically useful example, that relativistic particle-antiparticle (quasi-)bound states, viewed as photon-

photon resonances, can be conveniently and naturally treated by the variational method within the Hamiltonian formalism of quantum field theory. This formalism is eminently suited for a description of photon-photon scattering in the  $e^+e^-$  resonance region. To our knowledge this is the first time that resonance bound-state phenomena in QED and continuum scattering are presented in a unified manner. This is the main point of this investigation. In Sec. II we derive the integral equations that describe the coupled  $\gamma\gamma$  and  $e^+e^-$  channels, and outline their solution. The results are presented and discussed in Sec. III. Concluding remarks are given in Sec. IV.

### II. QED HAMILTONIAN, VARIATIONAL ANSATZ, AND EQUATIONS

The (normal-ordered) Hamiltonian operator of QED, written in the Coulomb gauge, is given by  $H = \int \mathcal{H} d^3x$ , where

$$\mathcal{H} = \mathcal{H}_0 + \mathcal{H}_C + \mathcal{H}_T, \quad (3)$$

$$\mathcal{H}_0 = \psi^\dagger (-i\boldsymbol{\alpha} \cdot \nabla + \beta m) \psi + \frac{1}{2} [ \dot{\mathbf{A}}^2 + (\nabla \times \mathbf{A})^2 ], \quad (4)$$

$$\mathcal{H}_C = \frac{e^2}{8\pi} \int d^3y \frac{\psi^\dagger(\mathbf{y}) \psi(\mathbf{y}) \psi^\dagger(\mathbf{x}) \psi(\mathbf{x})}{|\mathbf{x} - \mathbf{y}|}, \quad (5)$$

and

$$\mathcal{H}_T = -e\psi^\dagger \boldsymbol{\alpha} \cdot \mathbf{A} \psi. \quad (6)$$

In the Hamiltonian formalism we seek solutions of the equation

$$(H - E)|\psi\rangle = 0, \quad (7)$$

which follows from the variational principle

$$\langle \delta\psi | H - E | \psi \rangle = 0. \quad (8)$$

We consider approximate solutions of (7) based on the ansatz

$$\begin{aligned}
|\psi\rangle = & \sum_{s_1 s_2} \int d^3 p F_{s_1 s_2}(\mathbf{p}) b^\dagger(\mathbf{p}, s_1) d^\dagger(-\mathbf{p}, s_2) |0\rangle + \sum_{s_1 s_2 \lambda} \int d^3 p_1 d^3 p_2 G_{s_1 s_2 \lambda}(\mathbf{p}_1, \mathbf{p}_2) b^\dagger(\mathbf{p}_1, s_1) d^\dagger(\mathbf{p}_2, s_2) a^\dagger(\mathbf{p}_3, \lambda) |0\rangle \\
& + \sum_{\lambda_1 \lambda_2} \int d^3 p A_{\lambda_1 \lambda_2}(\mathbf{p}) a^\dagger(\mathbf{p}_1, \lambda_1) a^\dagger(\mathbf{p}_2, \lambda_2) |0\rangle, \tag{9}
\end{aligned}$$

where the functions  $F$ ,  $G$ , and  $A$  are adjustable coefficients, and  $\mathbf{p}_1 + \mathbf{p}_2 + \mathbf{p}_3 = 0$ . In Eq. (9),  $b^\dagger(\mathbf{p}, s)$  and  $d^\dagger(\mathbf{p}, s)$  are creation operators of free electrons and positrons with momentum  $\mathbf{p}$ , spin index  $s$  and mass  $m$ , corresponding to the free-particle Hamiltonian  $H_0$ , while  $a^\dagger(\mathbf{p}, \lambda)$  is the creation operator for photons of momentum  $\mathbf{p}$  and polarization index  $\lambda$ . The state  $|0\rangle$  is the vacuum eigenstate of  $H_0$ .

The above ansatz, which is sensitive to all terms in the Hamiltonian is a linear combination of two- and three-particle states. This ansatz will certainly not reproduce results of covariant perturbation theory, since to order  $\alpha^4$ , old-fashioned time-ordered perturbation theory requires multiparticle states that give the so-called “Z-graph” contributions. We have elaborated on this point in Ref. [6]. We emphasize, however, that resonance physics is an inherently nonperturbative phenomenon

and, in fact, the resonance height is *independent* of  $\alpha$ . Our ansatz is completely sufficient for our purposes as it includes the resonant channel. This channel completely dominates the cross section near resonance. In fact it will be shown (see Figs. 4 and 5) that the resonance sits on a background that lies nine orders of magnitude below. This background disagrees with covariant perturbation theory results by a factor of 2 as one would expect, due to the limitations of our ansatz. We should add that at very large  $\alpha$ , our results can only be considered illustrative as at high  $\alpha$  one expects dramatic changes to the vacuum state such as population by electron-positron pairs, for example.

Insertion of the ansatz (9) into the variational principle (8) results in the following set of coupled integral equations for the functions  $F$ ,  $G$ , and  $A$ :

$$\begin{aligned}
(2\omega_q - E)F_{s_1 s_2}(\mathbf{q}) - \frac{e^2}{(2\pi)^3} \sum_{s_3 s_4} \int d^3 p F_{s_3 s_4}(\mathbf{p}) \frac{1}{|\mathbf{p} - \mathbf{q}|^2} U_{q s_1}^\dagger U_{p s_3} U_{-p s_4}^\dagger V_{-q s_2} \\
- e \sum_{s_3 \lambda} \int d^3 p [G_{s_3 s_2 \lambda}(\mathbf{p}, -\mathbf{q}) U_{q s_1}^\dagger \boldsymbol{\alpha} \cdot \boldsymbol{\epsilon}_{\mathbf{q} - \mathbf{p}, \lambda} U_{p s_3} - G_{s_1 s_3 \lambda}(\mathbf{q}, -\mathbf{p}) V_{-p s_3}^\dagger \boldsymbol{\alpha} \cdot \boldsymbol{\epsilon}_{\mathbf{p} - \mathbf{q}, \lambda} V_{-q s_2}] = 0, \tag{10}
\end{aligned}$$

$$\begin{aligned}
G_{s_1 s_2 \lambda}(\mathbf{q}_1, \mathbf{q}_2) (\omega_{q_1} + \omega_{q_2} + |\mathbf{q}_1 + \mathbf{q}_2| - E) - e \sum_{s_3} [F_{s_3 s_2}(-\mathbf{q}_2) U_{q_1 s_1}^\dagger \boldsymbol{\alpha} \cdot \boldsymbol{\epsilon}_{-\mathbf{q}_1 - \mathbf{q}_2, \lambda} U_{-q_2 s_3} - F_{s_1 s_2}(\mathbf{q}_1) V_{-q_1 s_3}^\dagger \boldsymbol{\alpha} \cdot \boldsymbol{\epsilon}_{-\mathbf{q}_1 - \mathbf{q}_2, \lambda} V_{q_2 s_2}] \\
- e \sum_{\lambda_2} [A_{\lambda_2 \lambda}(\mathbf{q}_1 + \mathbf{q}_2) + A_{\lambda \lambda_2}(-\mathbf{q}_1 - \mathbf{q}_2)] U_{q_1 s_1}^\dagger \boldsymbol{\alpha} \cdot \boldsymbol{\epsilon}_{\mathbf{q}_1 + \mathbf{q}_2, \lambda_2} V_{q_2 s_2} = 0, \tag{11}
\end{aligned}$$

$$\begin{aligned}
(2|\mathbf{q}| - E) [A_{\lambda_2 \lambda_1}(\mathbf{q}) + A_{\lambda_1 \lambda_2}(-\mathbf{q})] - e \sum_{s_1 s_2} \int d^3 p [G_{s_1 s_2 \lambda_1}(\mathbf{p}, \mathbf{q} - \mathbf{p}) V_{\mathbf{q} - \mathbf{p}, s_2}^\dagger \boldsymbol{\alpha} \cdot \boldsymbol{\epsilon}_{\mathbf{q} \lambda_2} U_{p s_1} \\
+ G_{s_1 s_2 \lambda_2}(\mathbf{p}, -\mathbf{q} - \mathbf{p}) V_{-\mathbf{q} - \mathbf{p}, s_2}^\dagger \boldsymbol{\alpha} \cdot \boldsymbol{\epsilon}_{-\mathbf{q} \lambda_1} U_{p s_1}] = 0, \tag{12}
\end{aligned}$$

with  $\omega_q = \sqrt{\mathbf{q}^2 + m^2}$ ,  $\boldsymbol{\epsilon}_{\mathbf{k}\lambda} = [2|\mathbf{k}|(2\pi)^3]^{-1/2} \boldsymbol{\epsilon}'_{\mathbf{k}\lambda}$  and  $U_{p s} = \sqrt{m/\omega_p} u_{p s}$ , etc., where  $\boldsymbol{\epsilon}'_{\mathbf{k}\lambda}$  and  $u_{p s}$  are the usual photon polarization vectors and fermion spinors, respectively.

As the coupled equations (10) to (12) are quite complicated, we shall use an approximate decoupling scheme rather than solving them directly. Taking  $E = \omega_{q_1} + \omega_{q_2}$ , in lowest order, Eq. (11) provides us with an explicit expression for  $G_{s_1 s_2 \lambda}(\mathbf{q}_1, \mathbf{q}_2)$  in terms of  $F_{s_1 s_2}(\mathbf{q})$  and  $A_{\lambda_1 \lambda_2}(\mathbf{k})$ . We substitute this expression for  $G_{s_1 s_2}$  into (10) and obtain the equation

$$\begin{aligned}
(2\omega_q - E)F_{s_1 s_2}(\mathbf{q}) - \frac{e^2}{(2\pi)^3} \sum_{s_3 s_4} \int d^3 p F_{s_3 s_4}(\mathbf{p}) \frac{1}{|\mathbf{p} - \mathbf{q}|^2} K_{s_1 s_3 s_2 s_4}(\mathbf{q}, \mathbf{p}) \\
= e^2 \sum_{s_3 \lambda_1 \lambda_2} \int \frac{d^3 p}{|\mathbf{p} - \mathbf{q}|} [A_{\lambda_2 \lambda_1}(\mathbf{q} - \mathbf{p}) + A_{\lambda_1 \lambda_2}(\mathbf{p} - \mathbf{q})] U_{q s_1}^\dagger \boldsymbol{\alpha} \cdot \boldsymbol{\epsilon}_{\mathbf{q} - \mathbf{p}, \lambda_2} (U_{p s_3} U_{p s_3}^\dagger - V_{-p s_3} V_{-p s_3}^\dagger) \boldsymbol{\alpha} \cdot \boldsymbol{\epsilon}_{\mathbf{p} - \mathbf{q}, \lambda_1} V_{-q s_2}, \tag{13}
\end{aligned}$$

where

$$K_{s_1 s_3 s_2 s_4}(\mathbf{q}, \mathbf{p}) = U_{q s_1}^\dagger U_{p s_3} V_{-p s_4}^\dagger V_{-q s_2} - \sum_{\lambda} U_{q s_1}^\dagger \boldsymbol{\alpha} \cdot \boldsymbol{\epsilon}'_{\mathbf{q} - \mathbf{p}, \lambda} U_{p s_3} V_{-p s_4}^\dagger \boldsymbol{\alpha} \cdot \boldsymbol{\epsilon}'_{\mathbf{p} - \mathbf{q}, \lambda} V_{-q s_2}. \tag{14}$$

We note in passing that if  $A_{\lambda_1 \lambda_2}$  is set to zero, (13) reduces to an integral equation for relativistic fermion-antifermion

bound states derived earlier [7] using a more limited ansatz in which  $A_{\lambda_1\lambda_2} = 0$  in (9).

In arriving at Eq. (13) we implicitly added a mass counterterm to our original Hamiltonian. The counterterm was chosen to precisely cancel all self-energy contributions that arise from the Coulomb and transverse-photon interaction Hamiltonians. Mass renormalization is trivial at this level of inclusion of Fock-space states.

To complete the approximate decoupling, in Eq. (12), we make the lowest-order replacement

$$G_{s_1s_2\lambda}(\mathbf{q}_1, \mathbf{q}_2) \simeq \frac{e}{|\mathbf{q}_1 + \mathbf{q}_2|} \sum_{s_3} [F_{s_3s_2}(-\mathbf{q}_2) U_{q_1s_1}^\dagger \boldsymbol{\alpha} \cdot \boldsymbol{\epsilon}_{-\mathbf{q}_1 - \mathbf{q}_2, \lambda} U_{-q_2s_3} - F_{s_1s_3}(\mathbf{q}_1) V_{-q_1s_3}^\dagger \boldsymbol{\alpha} \cdot \boldsymbol{\epsilon}_{-\mathbf{q}_1 - \mathbf{q}_2, \lambda} V_{q_2s_2}] , \quad (15)$$

which transforms Eq. (12) into the form

$$(2|\mathbf{q}| - E) [A_{\lambda_2\lambda_1}(\mathbf{q}) + A_{\lambda_1\lambda_2}(-\mathbf{q})] \\ = \frac{e^2}{|\mathbf{q}|} \sum_{s_1s_2s_3} \int d^3p F_{s_1s_2}(\mathbf{p}) [V_{-qs_2}^\dagger \boldsymbol{\alpha} \cdot \boldsymbol{\epsilon}_{q\lambda_2} (U_{p+q,s_3} U_{p+q,s_3}^\dagger - V_{-p-q,s_3} V_{-p-q,s_3}^\dagger) \boldsymbol{\alpha} \cdot \boldsymbol{\epsilon}_{-q\lambda_1} U_{p,s_1} \\ + V_{-ps_2}^\dagger \boldsymbol{\alpha} \cdot \boldsymbol{\epsilon}_{-q\lambda_1} (U_{p-q,s_3} U_{p-q,s_3}^\dagger - V_{q-p,s_3} V_{q-p,s_3}^\dagger) \boldsymbol{\alpha} \cdot \boldsymbol{\epsilon}_{q\lambda_2} U_{p,s_1}] . \quad (16)$$

We note that the terms in parentheses on the right-hand side which also appear in Eq. (13) are the spin-projected covariant fermion propagators integrated over  $p_0$ .

Equations (13) and (16) couple the bound fermion-antifermion channels, described by the momentum-space wave functions  $F_{s_1s_2}(\mathbf{q})$ , to the two-photon channels, described by the coefficients  $A_{\lambda_1\lambda_2}(\mathbf{k})$ .

To proceed further we specify a particular  $J^{PC}$  state. We do this as in Ref. [7] and write

$$F_{s_1s_2}(\mathbf{p}) = F(p) \bar{U}_{ps_1} \Gamma V_{-ps_2} = F(p) g_{s_1s_2}(\mathbf{p}) , \quad (17)$$

where  $\Gamma$  is the appropriate Dirac matrix (e.g.,  $\Gamma = \gamma_5$  for the  $0^{+-}$  states). Also, making the substitution

$$a_{\lambda_2\lambda_1}(\mathbf{q}) = A_{\lambda_2\lambda_1}(\mathbf{q}) + A_{\lambda_1\lambda_2}(-\mathbf{q}) , \quad (18)$$

and performing the requisite matrix manipulations, we find that Eq. (16) becomes

$$(2|\mathbf{q}| - E) a_{\lambda_2\lambda_1}(\mathbf{q}) = \frac{e^2}{(2\pi)^3 |\mathbf{q}|^2} \int d^3p F(p) \frac{1}{\omega_p^2} t_{\lambda_2\lambda_1}(\mathbf{p}, \mathbf{q}) , \quad (19)$$

where

$$t_{\lambda_2\lambda_1}(\mathbf{p}, \mathbf{q}) = \frac{1}{8\omega_{p+q}} \text{tr}[(\not{p} + m) \Gamma (\not{\tilde{p}} - m) \boldsymbol{\epsilon}'_{q\lambda_2} (\not{p}' + \not{q}' + m) \boldsymbol{\epsilon}'_{-q\lambda_1}] + \frac{1}{8\omega_{p-q}} \text{tr}[(\not{p} + m) \Gamma (\not{\tilde{p}} - m) \boldsymbol{\epsilon}'_{-q\lambda_1} (\not{p}' - \not{q}' + m) \boldsymbol{\epsilon}'_{q\lambda_2}] , \quad (20)$$

where  $p = (\omega_p, \mathbf{p})$ ,  $\tilde{p} = (\omega_p, -\mathbf{p})$ ,  $p' = (0, \mathbf{p})$ , and  $\boldsymbol{\epsilon}'_{q\lambda} = (0, \boldsymbol{\epsilon}'_{q\lambda})$ .

The reduction of Eq. (13) proceeds similarly, and we obtain

$$(2\omega_p - E) F(p) g^2(p) - \frac{e^2}{(2\pi)^3} \int d^3p \frac{F(p)}{|\mathbf{p} - \mathbf{q}|^2} K(\mathbf{p}, \mathbf{q}) = \frac{e^2}{(2\pi)^3} T(\mathbf{q}) , \quad (21)$$

where

$$T(\mathbf{q}) = \sum_{\substack{\lambda_1\lambda_2 \\ s_1s_2}} g_{s_1s_2}^\dagger(\mathbf{q}) \int \frac{d^3p}{p^2 2\omega_{q-p}} a_{\lambda_2\lambda_1}(\mathbf{p}) \bar{U}_{qs_1} \boldsymbol{\epsilon}'_{p\lambda_2} (\not{Q}' + m) \boldsymbol{\epsilon}'_{-p\lambda_1} V_{-qs_2} , \quad (22)$$

with  $Q' = (0, \mathbf{q} - \mathbf{p})$ , and

$$K(\mathbf{p}, \mathbf{q}) \{ [\text{tr}[(\not{q}' - m) \bar{\Gamma} (\not{q}' + m) \gamma_\mu (\not{p}' + m) \Gamma (\not{p}' - m) \gamma^\mu] + \text{tr}[(\not{q}' - m) \bar{\Gamma} (\not{q}' + m) \eta (\not{p}' + m) \Gamma (\not{p}' - m) \eta] \} / 16\omega_q^2 \omega_p^2 \quad (23)$$

with  $\eta = \boldsymbol{\gamma} \cdot (\mathbf{q} - \mathbf{p}) / |\mathbf{q} - \mathbf{p}|$ , and

$$g^2(p) = \sum_{s_1s_2} |g_{s_1s_2}(\mathbf{p})|^2 = \frac{1}{4\omega_p^2} \text{tr}[\bar{\Gamma} (\not{p} + m) \Gamma (\not{p}^\dagger - m)] . \quad (24)$$

We next consider the coupled equations (19) and (21) for the specific case  $0^{-+}(^1S_0)$ . In doing so we will concentrate on the most salient feature of the present formalism, namely, the description of the  $e^+e^-$  (or  $\mu^+\mu^-$  etc.) electromagnetic bound state as a photon-photon resonance.

Consistent with our lowest-order approximation, we evaluate  $t_{\lambda_2\lambda_1}$  in the nonrelativistic limit:

$$t_{\lambda_2\lambda_1} = \frac{-2i(-1)^{\lambda_1}m^2}{\omega_q} \mathbf{q} \cdot \boldsymbol{\epsilon}'_{q\lambda_2} \times \boldsymbol{\epsilon}'_{q\lambda_1}. \quad (25)$$

Thus, we write

$$a_{\lambda_2\lambda_1}(\mathbf{q}) = -i(-1)^{\lambda_1} \frac{\mathbf{q}}{|\mathbf{q}|} \cdot \boldsymbol{\epsilon}'_{q\lambda_2} \times \boldsymbol{\epsilon}'_{q\lambda_1} a(q), \quad (26)$$

whereupon Eq. (19) for the  $0^{-+}$  state reduces in this approximation to the radial equation

$$(q - q_0)a(q) = \frac{2\alpha}{\pi} \frac{m^2}{q\omega_q} \int_0^\infty dp \frac{p^2}{\omega_p^2} \frac{f(p)}{g(p)}, \quad (27)$$

where  $\alpha = e^2/4\pi$ ,  $q = |\mathbf{q}|$  and  $E = 2q_0$ . We have written  $F(p) = g(p)f(p)$ , with  $g(p) = \sqrt{2}$  for the  $0^{-+}$  case.

This equation has the formal photon-photon scattering solution

$$a_{q_0} = \delta(q - q_0) + \frac{2}{q - q_0} \frac{\alpha}{\pi} \frac{m^2}{q\omega_q} \int_0^\infty dp \frac{p^2}{\omega_p^2} \frac{f(p)}{\sqrt{2}}, \quad (28)$$

where the coefficient of  $4/(q^2 - q_0^2)$  gives the  $0^{-+}$  partial  $K$  matrix [6]. In keeping with our lowest-order approximations, we evaluate Eq. (21) for the  $0^{-+}$  case, by substituting in only the first term of (28), i.e.,  $a_{q_0}(q) = \delta(q - q_0)$  into (26) and then the resulting  $T(\mathbf{q})$  of Eq. (22) into Eq. (21). The result is an inhomogeneous relativistic Schrödinger-like equation for the radial momentum-space  $0^{-+}$  wave function:

$$(2\omega_q - E)f(q) - \frac{\alpha}{\pi} \int_0^\infty dp \frac{p}{q} f(p) k(p, q) = \frac{2\alpha}{\pi} \frac{\sqrt{2}q_0 m}{\omega_q \omega_{q_0}}, \quad (29)$$

where

$$k(p, q) = \frac{(\omega_p + \omega_q)^2 + 4(\omega_p \omega_q - m^2)}{4\omega_p \omega_q} \times \ln \left| \frac{p+q}{p-q} \right| - \frac{pq}{2\omega_p \omega_q}. \quad (30)$$

Equations (28) and (29) represent our main result. From Eq. (28) we see that scattering of photons results as a consequence of a nonzero amplitude for an  $e^+e^-$  pair, i.e.,  $f(p)$ . Equation (29) shows that off resonance  $f(p)$  is essentially controlled by the inhomogeneous right-hand side. At particular  $E$  values the operator on the left-hand side of (29) becomes singular, resulting in very large values of  $f(p)$ , which, in turn, generate a resonant  $\gamma\gamma$  cross section.

Equation (29), with the inhomogeneous right-hand side set to zero, is a momentum-space relativistic eigenvalue

equation for  $e^+e^-$  bound states of  $0^{-+}$  symmetry, which we discussed earlier [7]. In the nonrelativistic limit this homogeneous equation is precisely the  $s$ -wave radial Schrödinger equation. However, the nonzero right-hand side of (29), which couples the  $e^+e^-$  system to the  $\gamma\gamma$  channel, implies that Eq. (29) has nontrivial solutions for all  $E > 0$ , and not just at the specific eigenenergies  $E \simeq 2m - m\alpha^2/4n^2$  ( $n=1,2,3,\dots$ ). This is consistent with the fact that QED has a purely continuous spectrum for all energies above the vacuum energy.

### III. RESULTS AND DISCUSSION

We solve the radial integral equation (29) numerically to obtain  $f(q)$  at a given  $E = 2q_0$ , as discussed in Ref. [6]. The momentum variable is mapped into a finite interval via the transformation  $p = \beta \tan(\theta)$ , where  $\beta$  is a scale parameter chosen as a multiple of the coupling constant  $\alpha$ . Equation (29) is converted into a set of linear algebraic equations by means of a Fourier-sine expansion of  $f(\theta)$ . These solutions are then used to evaluate the  $0^{-+}$   $K$  matrix element using the expression [cf. Eq. (28) with  $m=1$ ]

$$K_0 = \tan \eta_0 = \frac{2\alpha m^2}{q_0 \omega_{q_0}} \int_0^\infty dp \frac{p^2}{\omega_p^2} \frac{f(p)}{\sqrt{2}}, \quad (31)$$

and therefore the partial cross section

$$\sigma_{\gamma\gamma} = \frac{2\pi}{q_0^2} \sin^2 \eta_0. \quad (32)$$

Figures 1 and 2 are plots of this partial photon-photon cross section,  $\sigma_{\gamma\gamma}$  for two values of the coupling constant. The prominent resonances, which have maxima at the positions of the quasibound particle-antiparticle states, are evident in these plots. At low  $\alpha$  the positions of the maxima occur at  $E/m = 2 - \alpha^2/(4n^2) - (24 - 3/n)\alpha^4/(64n^3)$  as discussed in Ref. [7], augmented by an  $O(\alpha^5)$  shift due to the coupling to the photon-photon channel [8]. At the maximum, the cross section takes on its ‘‘unitary limit’’ value of  $\sigma_{\gamma\gamma} = 2\pi/q_0^2 \simeq 10^{-20}$  cm<sup>2</sup>. The shift in the position of the maximum of the cross section  $E_i$ , compared to the energy eigenvalues of Eq. (28) with the right-hand side set equal to zero, results as a consequence of the fact that the resonant part of the phase shift (which crosses  $\pi/2$  at  $E_i$ ) is added to a background phase.

The finite number of states kept in the Fourier expansion of the bound-state wave function limits our numerical results in that only the lowest three resonances (radial excitations) are properly represented. The calculations reported here were performed with about 30 Fourier states kept in the expansion and required little computer time.

For the case of  $\alpha=0.2$ , shown in Fig. 1, results from two calculations are given: in addition to the calculation with kernel (30), which includes both the Coulomb- and transverse-photon exchange interactions in the  $e^+e^-$  bound-state channel, a calculation with Coulomb-photon exchange only is presented. It can be seen that the main features are present in this calculation except that the

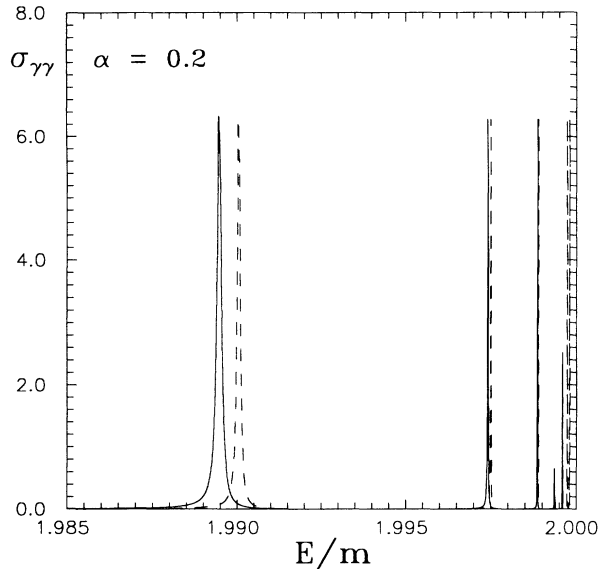


FIG. 1. Photon-photon scattering cross section in units of  $1/m^2$  as a function of total energy for a QED coupling constant of  $\alpha=0.2$ . Solid line: calculated with kernel (30), dashed line: no transverse-photon exchange in Eq. (29) included; see text.

resonance positions are shifted.

We have fitted a Breit-Wigner form to the resonance peaks and extracted the widths. A plot of these widths for the lowest-energy resonance ( $n=1$ ) is given in Fig. 3. We find that these widths follow the perturbative result [8],

$$\Gamma/m = \frac{1}{2}\alpha^5, \quad (33)$$

quite closely, even up to relative large values of  $\alpha$ , beyond which our results begin to deviate upwards from the perturbative values. For  $n > 1$  the widths are reduced by the

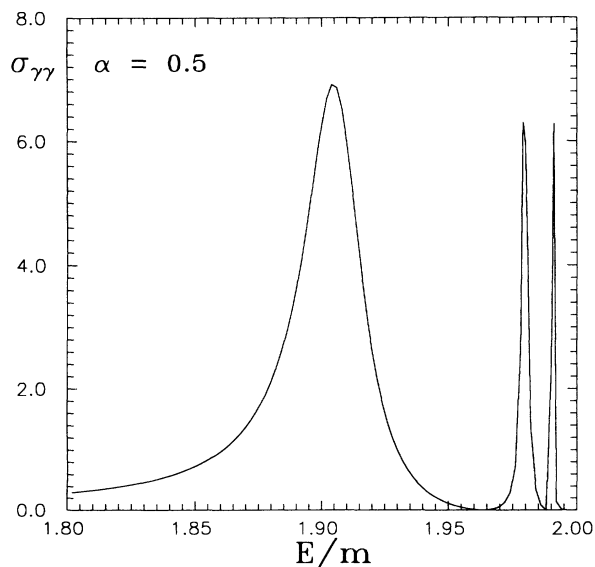


FIG. 2. Same as in Fig. 1 for  $\alpha=0.5$ . The strong deviation in the ground-state resonance position from the nonrelativistic value of  $E/m = 2 - \alpha^2/4 = 1.9375$  is obvious.

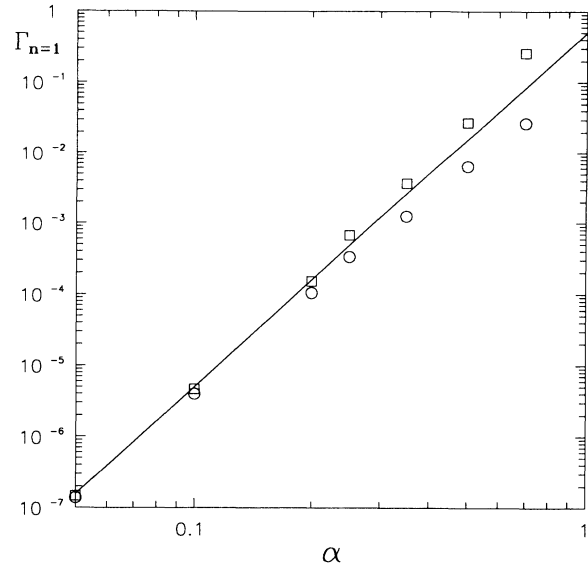


FIG. 3. Width of the ground-state resonance as a function of the QED coupling constant. Solid line: lowest-order perturbative result (33), circles: present result with Coulomb-photon exchange only, squares: present results including transverse-photon exchange (30).

well-known ( $1/n^3$ ) factor.

In principle there are infinitely many resonances, that crowd up against the “dissociation limit” at  $E=2m$ . In practice we are able to resolve only a few of the lower ones, due to the approximate numerical method we employ in solving Eq. (29).

For small values of  $\alpha$ , off resonance, where perturbation theory would be expected to hold, our predicted  $\sigma_{\gamma\gamma}$  elastic cross section behaves as  $\alpha^4 E^2$ , which is considerably larger than the familiar perturbative result  $\alpha^4 E^6$  [Eq. (1)]. This is because our ansatz (9) does not contain all the Fock-space states needed to reproduce perturbation theory at low order in  $\alpha$ . We could add these states, at considerable expense in complexity, but this would not change the results near resonance significantly. The resonance results are completely dominated by the channels which we have included in (9), and attain the “unitary limit” value of  $\sigma_{\gamma\gamma} = 2\pi/q_0^2$  independent of  $\alpha$ .

In Fig. 4 results are shown for  $\sigma_{\gamma\gamma}$  with the correct value of the fine-structure constant  $\alpha \approx 1/137$  in the vicinity of the positronium ground-state resonance. While the cross section rises by about ten orders of magnitude at the resonance, the width is also very small. Whether this resonance (or the sequence for  $n=1,2,3,\dots$ ) can be observed experimentally, given the energy resolution of currently available photon sources at these energies, is under investigation [9]. It should be noted that one does not require an energy resolution of the order of the width (33), i.e.,  $\Delta E = 10^{-5}$  eV, but that one has to discriminate energies on an interval where the cross section falls by many orders of magnitude. As is apparent from Fig. 4 a relative energy resolution of the order of  $10^{-7}$  or  $\Delta E = 0.1$  eV is required in order to detect the Breit-Wigner resonance.

Our calculation predicts structure in the cross section

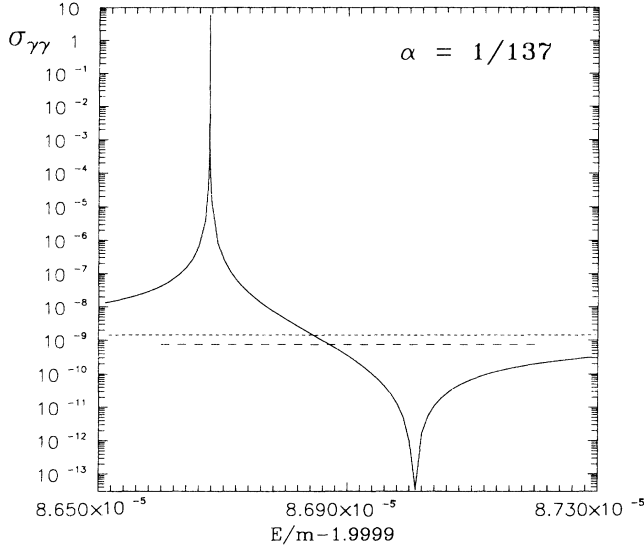


FIG. 4. Photon-photon scattering cross section for  $\alpha=1/137$  in the vicinity of the ground-state resonance. Solid line: present result with kernel (30), short dashed line: present result with kernel set equal to zero (no photon exchanges in virtual  $e^+e^-$  channel), long dashed line: perturbative result [3]. On the energy scale 1.9999 has been subtracted to facilitate the display of labels.

beyond the Breit-Wigner shape. We observe that the phase shift  $\eta_0$  rises by  $\pi$  radians at the ( $n=1$ )-resonance energy. The crossing of  $\eta_0=\pi$  gives rise to a drop of the partial cross section to zero and can be interpreted as a destructive interference between the resonating and background scattering contributions. We cannot be certain that the broad feature predicted by our calculation in the vicinity of the resonance is entirely correct. Due to the limited nature of our Fock-space ansatz (9) our calculation does not yield the results of covariant perturbation theory to order  $\alpha^4$  off resonance and is guaranteed to be exact only at resonance. In order to compare our calculation to the covariant perturbation theory result, which ignores the bound virtual positronium formation, but includes virtual formation of free  $e^+e^-$  pairs [4] and which rises steeply as the energy approaches  $2m$ , we have carried out a solution of Eqs. (28) and (29) with the photon exchange kernel (30) set equal to zero. This result is seen to be free of resonances. How real the enhancement of the cross section near the resonance is, will be the subject of a subsequent (much more complicated) calculation with enough Fock space included to ensure covariance at the required order of  $\alpha$ . The background scattering cross section from this calculation will agree with the covariant calculation not only in its energy dependence, but also in the absolute height of the cross section near  $E=2m$ .

Figure 5 shows our results for the  $n=2$  resonance. As expected the width is reduced by a factor of 8 compared to Eq. (33). The interference between the resonating and

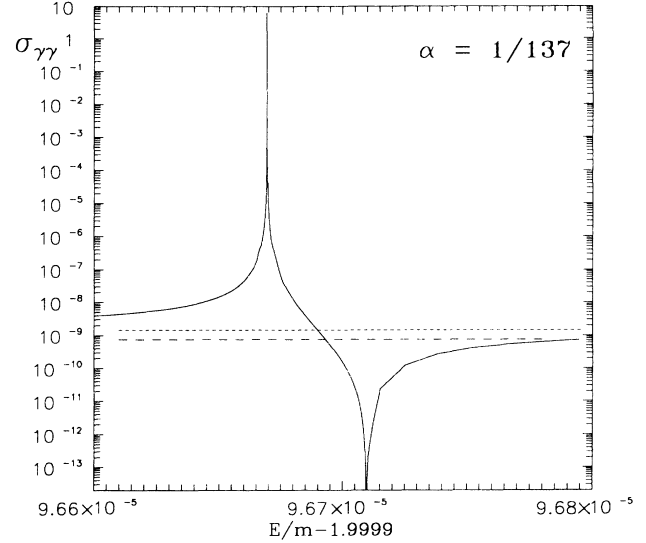


FIG. 5. Same as in Fig. 4, but for the  $n=2$  resonance. Note that the energy scale is stretched by a factor of 4 compared to Fig. 4.

continuous background part of the elastic photon-photon cross section happens closer to the resonance position. From this one can conclude a similar behavior for the higher- $n$  resonances of which there are infinitely many in between the position of the  $n=2$  resonance and the threshold for the creation of free  $e^+e^-$  pairs.

#### IV. CONCLUDING REMARKS

We have used a variational method in the Hamiltonian formalism of QED to derive coupled integral equations that describe unstable fermion-antifermion bound states as resonances in elastic photon-photon scattering. These equations were solved approximately for the  $J^{PC}=0^{-+}$  case, to yield the photon-photon cross section, for various values of the coupling constant  $\alpha$ . The cross section is dominated by resonance peaks that occur at values of the energy which are very close to the eigenenergies obtained in a traditional bound-state formalism. The width of the lowest-lying resonance is found to be close to the prediction of perturbation theory,  $\Gamma=\frac{1}{2}m\alpha^5$ , even for relatively large values of  $\alpha$ . The photon-photon elastic cross section reaches a peak value of  $\sigma_{\gamma\gamma}=2\pi/m^2\approx 10^{-20}$  cm<sup>2</sup> on resonance, which is many orders of magnitude above nonresonant perturbative values [Eq. (1)] and hence may be amenable to experimental observation.

#### ACKNOWLEDGMENTS

We thank Ted Barnes for a critical reading of the manuscript. The financial support of the Natural Sciences and Engineering Research Council of Canada is gratefully acknowledged.

- [1] R. S. Van Dyck, Jr., P. B. Schwinberg, and H. G. Dehmelt, *Phys. Rev. Lett.* **38**, 310 (1977).  
 [2] J. M. Jauch and F. Rohrlich, *The Theory of Photons and Electrons* (Addison-Wesley, Reading, MA, 1959), Chap.

13.  
 [3] W. Becker, J. K. McIver, and R. R. Schlicher, *J. Opt. Soc. Am. B* **6**, 1083 (1989).  
 [4] R. Karplus and M. Neumann, *Phys. Rev.* **83**, 776 (1951).

- [5] S. Ya Guzenko and P. I. Fomin, *Zh. Eksp. Teor. Fiz.* **47**, 2276 (1964) [*Sov. Phys. JETP* **20**, 1523 (1965)].
- [6] J. W. Darewych, M. Horbatsch, and R. Koniuk, *Phys. Rev. D* **42**, 4198 (1990).
- [7] W. Dykshoorn and R. Koniuk, *Phys. Rev. A* **41**, 64 (1990); J. W. Darewych and M. Horbatsch, *J. Phys. B* **23**, 337 (1990).
- [8] A. Rich, *Rev. Mod. Phys.* **53**, 127 (1981).
- [9] K. T. McDonald (private communication).